

Selfdiffusion in indium antimonide

Anjali Rastogi and K. V. Reddy

Citation: *J. Appl. Phys.* **75**, 4984 (1994); doi: 10.1063/1.355789

View online: <http://dx.doi.org/10.1063/1.355789>

View Table of Contents: <http://jap.aip.org/resource/1/JAPIAU/v75/i10>

Published by the [AIP Publishing LLC](#).

Additional information on J. Appl. Phys.

Journal Homepage: <http://jap.aip.org/>

Journal Information: http://jap.aip.org/about/about_the_journal

Top downloads: http://jap.aip.org/features/most_downloaded

Information for Authors: <http://jap.aip.org/authors>

ADVERTISEMENT



AIPAdvances

Now Indexed in
Thomson Reuters
Databases

Explore AIP's open access journal:

- Rapid publication
- Article-level metrics
- Post-publication rating and commenting

Self-diffusion in indium antimonide

Anjali Rastogi and K. V. Reddy

Department of Physics, Indian Institute of Technology, Madras, Madras 600 036, India

(Received 1 October 1993; accepted for publication 28 January 1994)

In the present paper indium and antimony self-diffusion was studied in the temperature range 400–500 °C in single crystals of indium antimonide. The crystals were grown by the Bridgman technique. The radioactive tracer diffusion method was employed using In^{114m} and Sb^{125} isotopes. Anodic oxidation technique was developed and used for serial sectioning. The penetration profiles were fitted to the error function solution of diffusion equations. For indium self-diffusion, the activation energy and pre-exponential factor were found to be 1.45 eV and $6.0 \times 10^{-7} \text{ cm}^2/\text{s}$, respectively, while for antimony diffusion the activation energy was obtained as 1.91 eV with a pre-exponential factor of $5.35 \times 10^{-4} \text{ cm}^2/\text{s}$. The results were compared with the earlier experimental studies and theoretical calculations. The migration enthalpies of indium and antimony atoms are estimated to be 0.66 and 0.70 eV, respectively. The corresponding formation enthalpies are 0.79 eV for In vacancy and 1.21 eV for Sb vacancy formation.

I. INTRODUCTION

The development of numerous semiconductor devices for various applications requires semiconductor materials of varied band-gap energies. A complete understanding of electrical and mass transport properties is essential for the design, fabrication, and reliable operation of any device made using these materials. Although Si and GaAs are the two materials which are extensively used, one of the III-V compounds InSb is also an important material which finds application in Hall probes and IR detectors. One of the major drawbacks with III-V compound semiconductors is the degradation due to the loss of the group V element during device fabrication and usage. Mass transport, by self-diffusion and dopant ion transport, takes place due to the point defects present in the crystal. In a recent review Gosele and Tan¹ emphasized the need for reliable experimental data to understand the self-diffusion and some anomalous diffusion in III-V compounds. An important question raised in the review is about self-diffusion coefficients being of the same order of magnitude for group III and group V elements in intrinsic GaAs. It will be interesting to examine if the same holds true in the other III-V compounds also.

The experimental data on self-diffusion in III-V compounds are reviewed by Sharma.² It appears that the activation energies for group V elements are generally higher than that for group III elements in these compounds. In the case of InSb the activation energies for self-diffusion of In and Sb reported by different workers^{3–5} vary so much that it is difficult to choose definite values. Even the theoretical reports^{6–8} are not assertive about their calculations in view of the multitude of point defects present in these crystals. Another factor, which influences self-diffusion, particularly in InSb is the presence of a large dislocation density compared to other III-V compounds.⁹

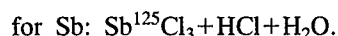
Self-diffusion coefficients are generally determined using radioactive tracers. The accuracy of the estimated values of the diffusion coefficients depends to a large extent on the method employed for sectioning the diffused samples. In the present work we measured the self-diffusion coefficients of

In and Sb in InSb single crystals, using radioactive tracers and anodic oxidation sectioning method. In analyzing the concentration profiles, the contribution due to the presence of dislocation is subtracted and the values of the self-diffusion coefficients are determined. The possible mechanism of mass transport is also discussed.

II. EXPERIMENTAL DETAILS

Indium antimonide crystals used in the present study were grown by vertical Bridgman method. The room-temperature carrier concentration of the crystals was of the order of 10^{14} cm^{-3} . High-purity (5 N) indium and antimony were used for the crystal growth. From the ingot 12-mm-diam and 2-mm-thick slices were cut. These were lapped on fine grade polishing paper and were further polished using diamond paste of grain sizes starting from 15 down to 0.25 μm till a highly reflecting mirror-like surface resulted. Samples were cleaned in trichloroethylene, acetone, dilute HF, and de-ionized water sequentially. It was followed by chemical polishing using a $\text{HF}:\text{HNO}_3:\text{H}_2\text{O}$ solution in 2:1:3 ratio. The samples were finally cleaned with de-ionized water and dried under a jet of argon gas.

Radioactive isotopes In^{114m} (half life 49.5 days) and Sb^{125} (half life 2.7 years) were used for self-diffusion study. Isotopes were supplied by Bhabha Atomic Research Centre, Bombay. A thin layer of the isotope was electroplated on the samples. The electrolytes used for this purpose were



The thickness of the overlayer was less than a monolayer for Sb and nearly 70 Å for In isotopes. The absolute surface activity for In samples was 20 000 counts/min and that for antimony 6000 counts/min as compared to the background activity of 15 counts/min. The samples were placed with their active surface covered by a clean oxidized silicon wafer of the same size and were wrapped in aluminum foil in order to avoid the evaporation losses. (Some of the diffusion runs were done in high-purity argon gas flow but the surface lost

its initial luster and was not useful for further studies.) The samples were then placed in an evacuated quartz cell which was flushed several times with hydrogen gas. It was finally evacuated to a vacuum of 10^{-5} Torr and partially filled with hydrogen gas such that, at annealing temperatures, the pressure inside the cell was less than one atmosphere. The temperature of the furnace was controlled using a PID controller to ± 0.1 °C and it was measured using a chromel-alumel thermocouple placed very close to the sample. Diffusion annealing was done for 24–45 h for indium diffusion runs and for 24–72 h for antimony diffusion runs. The temperature range studied was 400–500 °C. After diffusion the samples were still highly reflecting and no surface damage was observed when viewed by optical microscope under the magnification of 1000 \times (model Leitz LABORLUX 12 ME). However, above 500 °C the samples were found to be plastically deformed. After diffusion, the sides of the samples were ground off in order to remove any activity present due to surface migration. Samples were then cleaned and used for sectioning.

Electrochemical sectioning (anodic oxidation) is preferred to grinding as it enables one to remove material of desired thickness exactly parallel to the surface, and it causes least surface damage. The electrolyte used was prepared by taking a 3.5% solution of tartaric acid buffered with ammonia solution to pH=6.0. It was mixed with ethylene glycol in 1:3 volume ratio.¹⁰ A platinum foil was used as counter electrode. Anodic oxidation was done under constant current conditions and oxide thickness was measured using ellipsometry. A calibration curve giving the oxide thickness as a function of final voltage was prepared and used to estimate the thickness of the material removed during serial sectioning.¹¹ A constant current of about 3 mA/cm² was passed during the growth of the oxide layer. The final voltage ranged from 6 to 9 V oxidizing 100–150 Å thickness layers of InSb. A 100-Å-thick oxide layer is equivalent to a 89-Å-thick layer of InSb.

Near the surface 100-Å-thick layers and in deeper regions 150-Å-thick layers were removed. Nearly 25–30 oxidations were done till the radioactivity of the sections reached almost the background activity. Each time the oxide layer was etched out by one or two drops of dilute HF and the solution was collected on a plastic plate. One drop of the KOH solution was added to it for neutralization. These sections were then dried under a lamp.

A GM counter (Nucleonix model GC 601) was used to count the radioactivity present in each section. Counting was done for at least 20 min to reduce errors of statistical fluctuations. The radioactivity C , measured in each section removed, is proportional to the concentration of the diffusant. The relative concentration of the diffusant at different depths C/C_0 , where C_0 is the radioactivity in the first layer removed, is plotted as a function of the distance (x) of the layer from the surface to obtain the penetration profiles.

III. RESULTS

Indium and antimony self-diffusion studies were carried out in the temperature range 400–500 °C. The full penetration profiles for indium diffusion are shown in Fig. 1 and

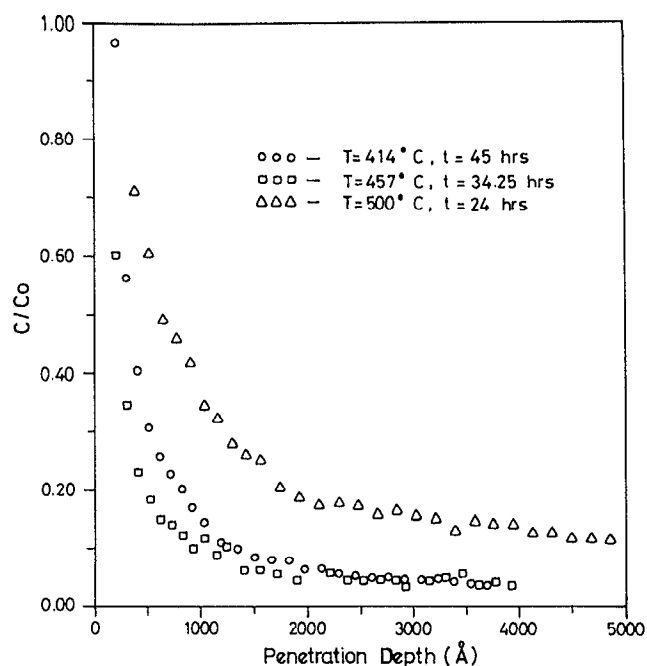


FIG. 1. Representative plots of relative concentration vs penetration depth for indium self-diffusion.

those for antimony in Fig. 2. For the sake of clarity only three profiles are plotted in each case. Figure 3 shows $\log C/C_0$ vs x plot for one of the representative diffusion profiles. It may be noticed that in the deeper region a straight line behavior can be seen which is characteristic of the presence of dislocations.¹² Some of the annealed samples were etched using the etchant 9HNO₃:5HF:1CH₃COOH:10H₂O for 10–15 s. The presence of dislocations, of the order of

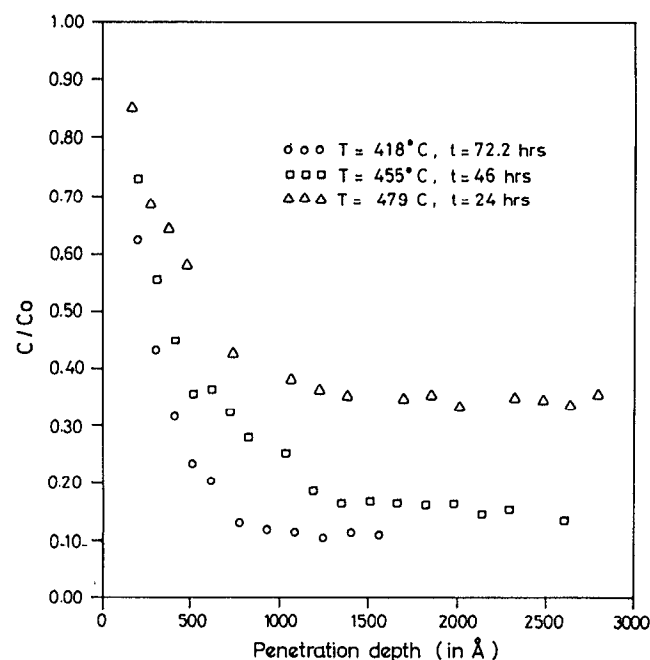


FIG. 2. Representative plots of relative concentration vs penetration depth for antimony self-diffusion.

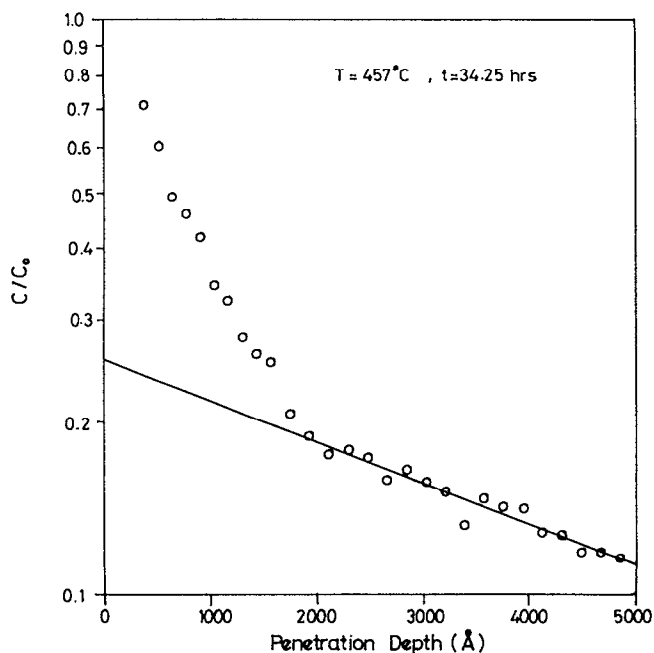


FIG. 3. Relative concentration vs penetration depth for indium diffusion at 457 °C and annealing time 34.25 h. The straight line region represents the dislocation contribution to migration of indium.

10^2 – 10^3 cm^{-2} , was observed. The actual concentration of dislocations may be larger since all of them are not revealed during preferential etching. The contribution from the dislocations was subtracted from the original curve by extrapolating the straight line to the surface region and subtracting the extrapolated concentration from the measured concentrations. The difference was again plotted as relative activity versus x plots. The corrected profiles in both the cases of indium as well as antimony self-diffusion were fitted to a complementary error function even though the thickness of the ^{125}Sb isotope deposited was less than a monolayer. Le Claire and Rabinovitch¹³ showed that even for the case of sufficiently thin source, depending on the solubility of the diffusant, time of annealing, and the temperature, the resulting profile follows either a Gaussian or an error function. Our data showed a better fit using error function rather than a Gaussian solution. The concentration of diffusant at any distance x from the surface, at time t is given by the equation¹⁴

$$C(x,t) = C_0 \operatorname{erfc}(x/2\sqrt{Dt}), \quad (1)$$

where C_0 is the concentration of the tracer on the surface, which remains nearly constant, and D is the diffusion coefficient. The error function fits for few temperatures are shown in Fig. 4 and Fig. 5 for In and Sb diffusion, respectively.

The experimental D values obtained from the least-squares fit of the corrected profiles at various temperatures studied for indium diffusion are listed in Table I. The Arrhenius plot (Fig. 6) for indium self-diffusion in InSb could be fitted to a single straight line given by

$$D(\text{cm}^2/\text{s}) = 6.0 \times 10^{-7} \exp[-(1.45 \pm 0.09) \text{ eV}/kT]. \quad (2)$$

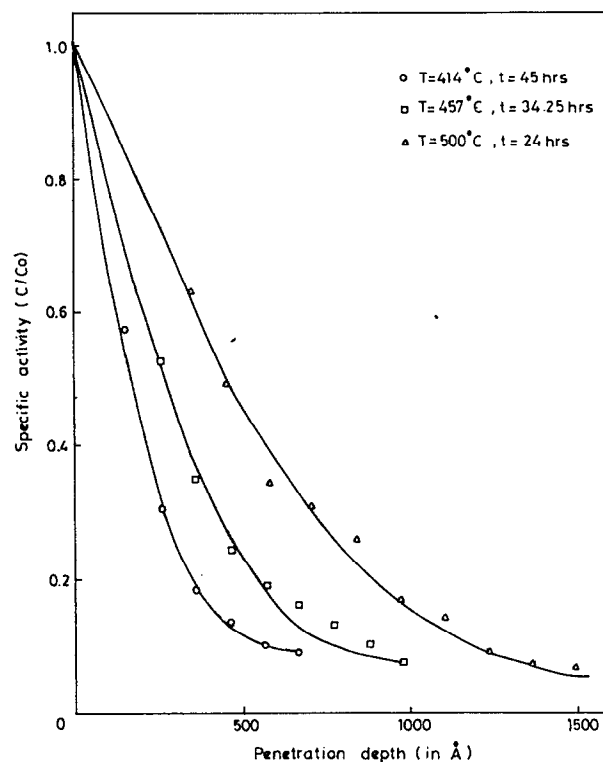


FIG. 4. Indium penetration profiles after subtracting the contribution due to dislocations. Solid lines represent the error function fit.

The diffusion coefficient values for antimony self-diffusion are listed in Table II. These values are slightly lower than the indium diffusion coefficients at the same temperature. The Arrhenius plot of Sb diffusion is also shown in Fig. 6. The data can be fitted to a straight line given by

$$D(\text{cm}^2/\text{s}) = 5.35 \times 10^{-4} \exp[-(1.91 \pm 0.08) \text{ eV}/kT]. \quad (3)$$

IV. DISCUSSION

It is well known that self-diffusion coefficients can best be determined by the use of radioactive tracers and serial sectioning. The accuracy of the self-diffusion coefficient values determined depends to a large extent on the methods employed for serial sectioning. In determining the diffusion profiles, better accuracy is obtained when the radioactivity in the sectioned portions is measured rather than the measurement of the residual activity in the specimen after each section is removed. Further, when the diffusion depths are shallow (less than one micron) the anodic oxidation sectioning is much more accurate compared to grinding.

Self-diffusion in InSb was first studied by Eisen and Birchenall.³ They used radioactive tracers but sectioning was done by grinding and the diffusion profiles were obtained by measuring the residual activity. The temperature range studied was 478–520 °C. Kendall and Huggins⁴ also studied self-diffusion in InSb in the same temperature range. They studied diffusion at three different temperatures and observed that at the highest temperature surface melting takes place. Another serious error in the measurement was that the sec-

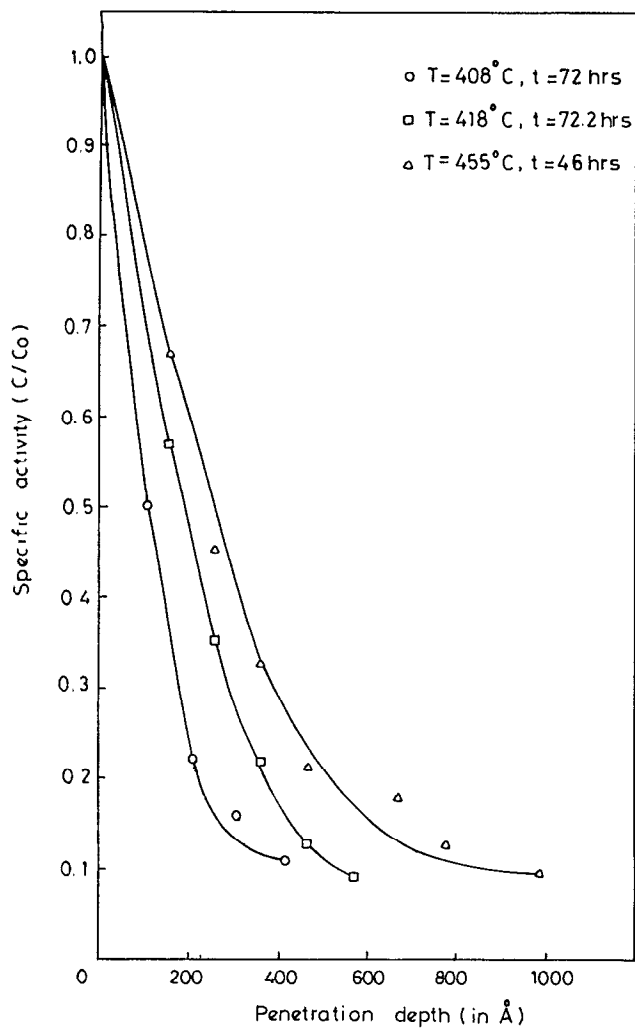


FIG. 5. Antimony penetration profiles after subtracting the contribution due to dislocations. Solid lines represent the error function fit.

tions ground off each time were of the same order as \sqrt{Dt} , where D is the diffusion coefficient and t is the time of anneal.

Siethoff⁵ analyzed the plastic deformation data of Schaffer *et al.*¹⁵ in the temperature range 280–510 °C. The self-diffusion parameter was evaluated using the equation

$$\left(\frac{\tau_{iii}}{G}\right)^n = \left(\frac{kT\dot{\epsilon}_{iii}}{AD_0Gb}\right) \exp \frac{Q_{sd}}{kT}, \quad (4)$$

TABLE I. Temperature dependence of self-diffusion coefficient for In^{114m} in InSb crystals.

S. No.	Temperature (°C)	Time of anneal (h)	Diffusion coefficients D (10^{17}) cm^2/s
1	414	45.0	1.5 ± 0.1
2	435	30.0	3.6 ± 0.3
3	449	27.0	4.8 ± 0.4
4	457	34.25	5.6 ± 0.4
5	477	24.0	8.9 ± 0.7
6	500	24.0	24.3 ± 1.9

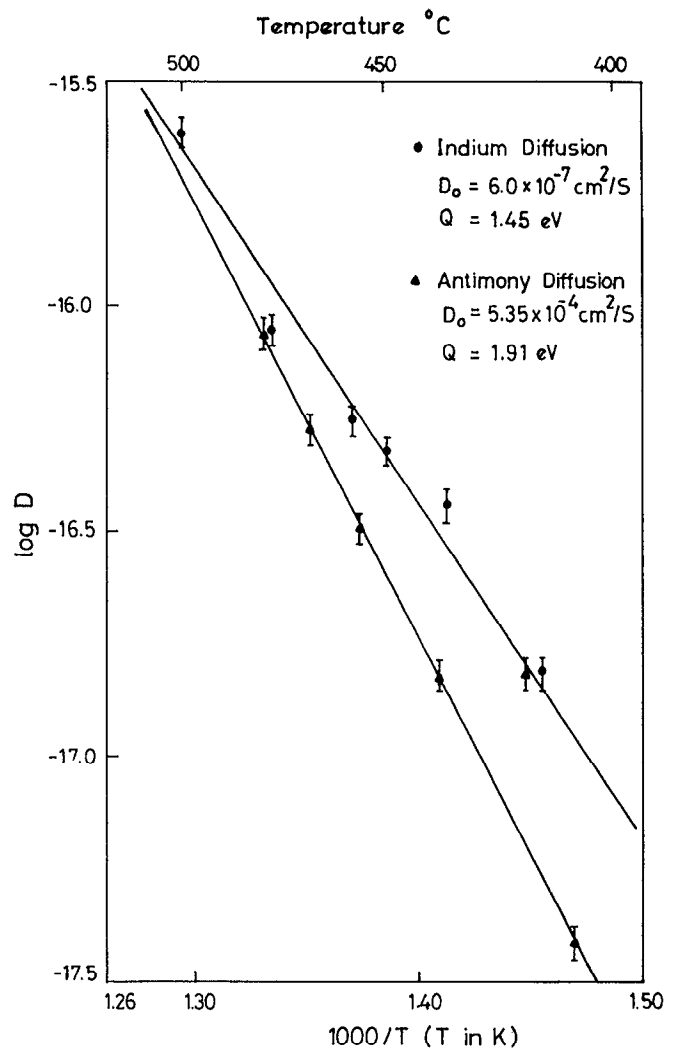


FIG. 6. Arrhenius plots for indium and antimony self-diffusion in InSb single crystals.

where τ_{iii} is shear stress, G is shear modulus, $\dot{\epsilon}_{iii}$ is strain rate, n and A are constants given by the relation $n=3.0 + 0.31 \log A$, b is Burgers vector, k is Boltzmann constant, D_0 is self-diffusion pre-exponential factor, and Q_{sd} is the activation energy. The self-diffusion activation energy obtained using this formula was 1.5 eV. It is not very clear if this activation energy corresponds to In migration or Sb migration.

TABLE II. Temperature dependence of self-diffusion coefficients for Sb¹²⁵ in InSb crystals.

S. No.	Temperature (°C)	Time of anneal (h)	Diffusion coefficients D (10^{17}) cm^2/s
1	408	72.0	0.39 ± 0.03
2	418	72.2	1.2 ± 0.1
3	436	72.0	1.5 ± 0.1
4	455	46.0	3.2 ± 0.3
5	467	24.0	5.3 ± 0.4
6	479	24.0	8.7 ± 0.7

TABLE III. Self-diffusion in InSb crystals (experimental data).

S. No.	Authors	Technique	Temp. range (°C)	Diffusant	D_0 (cm ² /s)	Q (eV)
1	Eisen and Birchenall ^a	Radiotracer	478–520	In	5×10^{-2}	1.82
				Sb	5×10^{-2}	1.94
2	Kendall and Huggins ^b	Radiotracer	475–517	In	1.8×10^{13}	4.3
				Sb	3.1×10^{13}	4.3
3	Present work	Radiotracer	414–500 408–479	In	6×10^{-7}	1.45
				Sb	5.35×10^{-4}	1.91

^aSee Ref. 3.

^bSee Ref. 4.

The experimental data already published together with the present work are summarized in Table III. The Arrhenius plots for In self-diffusion and Sb self-diffusion are plotted in Figs. 7 and 8 respectively for comparison.

It may be noted that the temperature range in the present work is almost twice that of the other two measurements.^{3,4} However, the present measurements are restricted to temperatures below 500 °C. At temperatures above 500 °C, we observed noticeable damage to the surface, thus conforming to the observations of Kendall and Huggins.⁴ In view of the shallow depths of diffusion profiles it is not advisable to analyze the diffusion profiles on surface damaged samples. The lower-temperature range in the present study could be extended mainly because anodic oxidation sectioning was

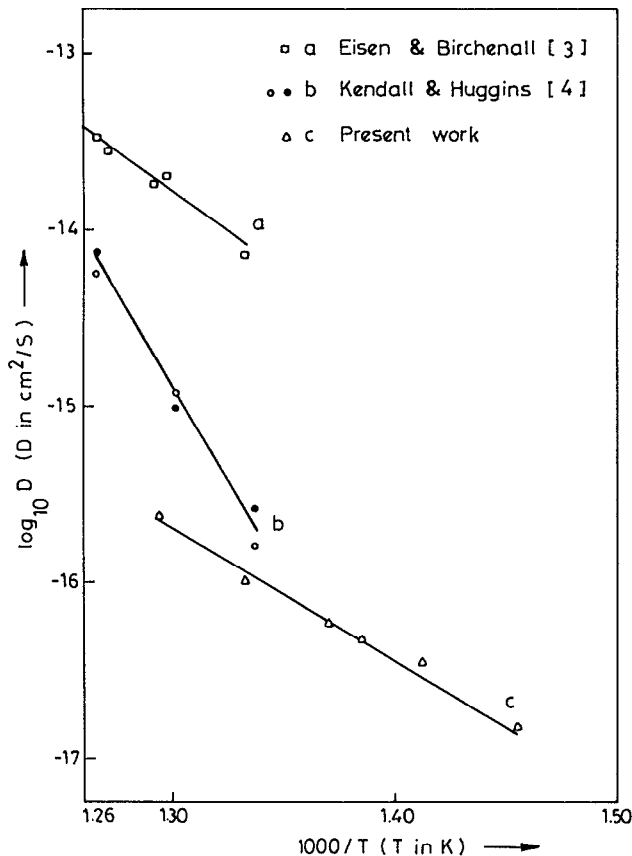


FIG. 7. Comparison of In self-diffusion data of the present work with the previously reported data.

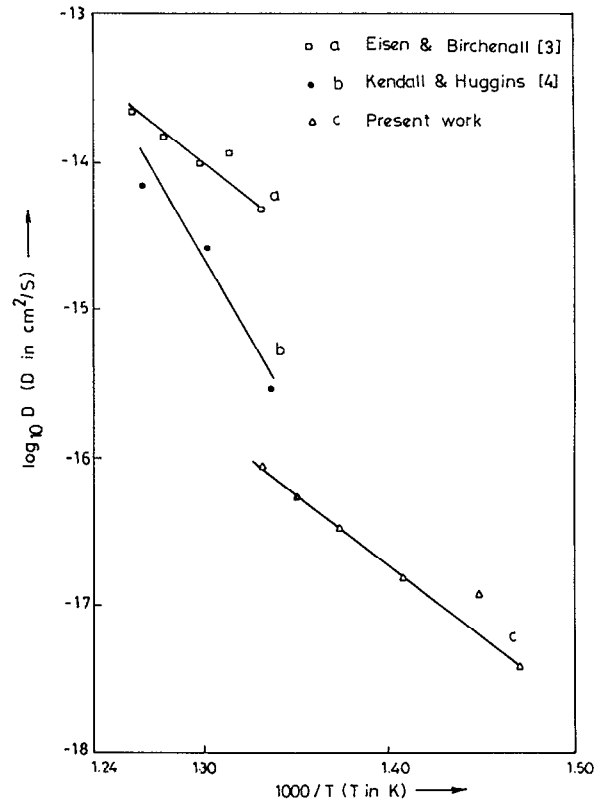


FIG. 8. Comparison of Sb self-diffusion data of the present work with the previously reported data.

employed instead of grinding. By this method, D values down to 10^{-17} cm²/s could be determined accurately. It is worth mentioning that the present study has yielded most reliable data on self-diffusion of In and Sb in InSb single crystals.

The activation energy for self-diffusion of In in InSb crystals was estimated to be 1.45 eV in the present work. Eisen and Birchenall³ obtained a value of 1.82 eV while Kendall and Huggins⁴ reported a value of 4.3 eV. It may be noted that in the latter case the experiment was done only at three temperatures and according to the authors' own observation the crystal surface was damaged during annealing at higher temperatures. The actual value of the diffusion coefficient measured by Kendall and Huggins at the lowest of the three temperatures is close to the value obtained in the present work (Fig. 7). This is understandable as in the analysis of diffusion profiles the contribution from dislocations was subtracted in both cases. The data of Eisen and Birchenall is about two orders of magnitude higher as they have not subtracted the dislocation contribution.

Copper diffusion in InSb crystals was studied by Stocker.¹⁶ By careful measurements it was shown that the diffusion coefficient is independent of dislocation concentration in crystals with dislocation density less than 10^3 . For crystals with a dislocation density greater than 10^3 , the diffusion coefficient increases steeply together with an increase in the density of dislocations. This could also be one of the possibilities for the high values of diffusion coefficient (Fig. 7) obtained by Eisen and Birchenall.³

Similar arguments hold good for Sb self-diffusion in InSb crystals. The activation energy obtained for Sb in the present work 1.91 eV is in close agreement with 1.94 eV reported by Eisen and Birchenall.³ Kendall and Huggins, however, reported that the activation energies for self-diffusion of In and Sb in InSb crystals are the same and equal to 4.3 eV. It may be pointed out that the close agreement in the activation energy for self-diffusion of Sb in InSb crystals, in the present work and that of Eisen and Birchenall,³ is not surprising since the presence of the dislocations only enhances the diffusion coefficient through pre-exponential factor and does not affect the activation energy. The activation energies obtained in the present work may be used to examine the mechanism of self-diffusion.

Lattice vacancies and interstitials are the defects in single crystals largely responsible for the mass transport due to self-diffusion. However, in III-V compound semiconductors, antisite defects may also contribute significantly to mass transport.¹⁷ From the measured activation energies for self-diffusion of In and Sb in InSb crystals we try to examine the possible mechanism of self-diffusion. It may be noted from the calculation of Van Vechten⁶ that in all III-V compounds interstitial defect formation energies are greater than vacancy formation energies. Assuming that self-diffusion takes place by monovacancy migration, migration enthalpies were calculated for the nearest-neighbor jump and the second nearest-neighbor jump by using the expression given by Van Vechten.¹⁸ The migration enthalpies favor the nearest-neighbor jump by the creation of antisite defects. This is similar to the results obtained for In self-diffusion in InP.¹⁹

The activation energies of indium and antimony self-diffusion obtained in the present study are 1.45 and 1.91 eV, respectively. The calculated migration enthalpies (ΔH_m) for a nearest-neighbor jump for In and Sb atoms are 0.66 and 0.70 eV, respectively. Assuming that the activation energy represents the sum of formation and migration enthalpies, the formation enthalpies of monovacancy are estimated to be 0.79 eV for In and 1.21 eV for Sb. Here it may be noted that the antimony vacancy formation enthalpy is more than that for indium vacancy. This is in conformity with the trend observed for III-V compounds.⁷

The pre-exponential factors obtained in the present study are rather low but not uncommon. Palfrey *et al.*²⁰ observed D_0 values of 4×10^{-5} cm²/s for Ga self-diffusion in GaAs. In CdSe these values were of the order of 10^{-2} – 10^{-3} cm²/s for Cd and Se self-diffusion²¹ while in the case of self-diffusion

in HgTe, which has almost the same band gap as InSb, D_0 values were reported to be 2×10^{-8} and 1×10^{-6} cm²/s respectively for Hg and Te diffusion.²² Kendall and Huggins⁴ have calculated D_0 values for InSb and showed that for sublattice vacancy migration the order of magnitude of D_0 is ~ 20 cm²/s while that for divacancy migration it is 10^{12} cm²/s. This shows that the diffusion mechanism in the present case is not vacancy migration in its own sublattice. The other possible migration is via antisite formation. Both activation energy values and pre-exponential factors support the formation of antisites which aid self-diffusion.

ACKNOWLEDGMENTS

We wish to thank Professor K. N. Bhat and P. R. S. Rao of the Electrical Engineering Department for their help in the thickness measurement using an ellipsometer and S. Mohan of the Humanities and Social Sciences Department for his valuable suggestions to improve the text.

- ¹U. Gosele and T. Y. Tan, *Defect and Diffusion Forum* **83**, 189 (1992).
- ²B. L. Sharma, *Defect and Diffusion Forum* **64-65**, 1 (1989).
- ³F. H. Eisen and C. E. Birchenall, *Acta Metall.* **5**, 265 (1957).
- ⁴D. L. Kendall and R. A. Huggins, *J. Appl. Phys.* **40**, 2750 (1969).
- ⁵H. Siethoff, *Phys. Lett.* **71A**, 265 (1979).
- ⁶J. A. Van Vechten, in *Handbook on Semiconductors*, edited by S. P. Keller (North Holland, New York, 1980), Vol. 3, p. 1.
- ⁷Y. M. Gu, L. Fritsche, and N. E. Christensen, *Phys. Status Solidi B* **159**, 617 (1990).
- ⁸T. W. Dobson and J. F. Wager, *J. Appl. Phys.* **66**, 1997 (1989).
- ⁹E. N. Pugh and L. E. Samuels, *J. Appl. Phys.* **35**, 1966 (1964).
- ¹⁰X. Tang, R. G. van Welzenis, F. M. van Setten, and A. J. Bosch, *Semicond. Sci. Technol.* **1**, 355 (1986).
- ¹¹A. Rastogi and K. V. Reddy, paper presented at First East West International Convention on Surface Engineering, Bangalore, India, December 16–19, 1992.
- ¹²A. D. Le Claire and A. Rabinovitch, *J. Phys. C* **14**, 3863 (1981).
- ¹³A. D. Le Claire and A. Rabinovitch, in *Diffusion in Crystalline Solids*, edited by G. E. Murch and A. S. Nowick (Academic, New York, 1984), pp. 264–265.
- ¹⁴P. G. Shewmon, in *Diffusion in Solids* (McGraw-Hill, New York, 1963), p. 14.
- ¹⁵S. Schafer, H. Alexander, and P. Haasen, *Phys. Status Solidi* **5**, 247 (1964).
- ¹⁶H. J. Stocker, *Phys. Rev.* **130**, 2160 (1963).
- ¹⁷J. A. Van Vechten, *Czech. J. Phys. B* **30**, 388 (1980).
- ¹⁸J. A. Van Vechten, *Phys. Rev. B* **12**, 1247 (1975).
- ¹⁹J. A. Van Vechten and J. F. Wager, *J. Appl. Phys.* **57**, 1956 (1985).
- ²⁰H. D. Palfrey, M. Brown, and A. F. W. Willoughby, *J. Electrochem. Soc.* **128**, 2224 (1981).
- ²¹Z. Zmija, *Acta Phys. Polonica A* **40**, 435 (1971).
- ²²F. A. Zaitov, V. I. Stafeev, and G. S. Khodakov, *Sov. Phys. Solid State* **14**, 2628 (1973).